A Diagnostic Case Study on the Comparison Between the Frontal and Non-Frontal Convective Systems*

ZHANG Xiaohui[1,2†] (张晓惠) and NI Yunqi[3] (倪允琪)

1 *College of Atmospheric Sciences, Nanjing University, Nanjing* 210093

2 *College of Earth Science, Graduate University of Chinese Academy of Sciences (GUCAS), Beijing* 100049

3 *State Key Laboratory of Severe Weather, Chinese Academy of Meteorological Sciences (CAMS), Beijing* 100081

(Received April 27, 2009)

ABSTRACT

Two major mesoscale convective clusters of different characters occurred during the heavy rainfall event in Guangxi Region and Guangdong Province on 20 June 2005, and they are preliminarily identified as a frontal mesoscale convective system (MCS1; a frontal cloud cluster) and a non-frontal MCS (MCS2; a warm sector cloud cluster). Comparative analyses on their convective intensity, maintenance mechanism, and moist potential vorticity (MPV) structure were further performed. The convective intensity analysis suggests that the ascending motion in both the frontal MCS1 and the warm sector MCS2 was strong, so it is hard to conclude whether the intensity of the frontal convective cluster was stronger than that of the non-frontal convective cluster, and their difference in precipitation might result from differences in their moisture conditions. The comparative analysis of the maintenance mechanisms of matured MCS1 and MCS2 show that in MCS1 there were strong northerly inflows at middle and upper levels, and the convection was mainly maintained through convective-symmetric instability; while in MCS2, the water vapor was abundant, and the convection was maintained by moist convective instability. The structural analysis of MPV indicates that (1) the two clusters were both potentially symmetric unstable at middle and low levels; (2) there were interactions between the cold/dry air and the warm/wet air in the frontal MCS1, and the interactions between the upper- and low-level jets in the warm sector MCS2; (3) the high- and low-level jets and moisture condition nearby the convective clusters exerted different impacts on the two types of convective systems, respectively.

Key words: South China, mesoscale convective system (MCS), convective instability, inertial instability, convective-symmetric instability, moist potential vorticity (MPV)

Citation: Zhang Xiaohui and Ni Yunqi, 2010: A diagnostic case study on the comparison between the frontal and non-frontal convective systems. *Acta Meteor. Sinica*, **24**(1), 66–77.

1. Introduction

The first rainy season in South China is usually considered as an important beginning of rainy seasons in summer. It is a special rainy season characterized by high occurrence frequency and long life duration of heavy rain, unique orographic effect, and overly abundant moisture conveying.

The quasi-stationary front is one kind of circulation system which occurs and develops all the year around South China. It is always recognized as strip-shaped clouds in the background of weak surface pressure fields (Li et al., 1984). It is believed that the quasi-stationary front which often induces heavy rain is related to symmetric instability in theory (Zheng, 1990). In addition, severe convection involving quasi-stationary front and instability were discussed by Ji et al. (2004). The mesoscale convective rainy clusters are the direct contributor to heavy rainfall. The trump-shaped terrain in the Nanling Mountains enhances the ascending motion of the warm and wet air from the south (Xia et al., 2006).

*Supported by the National "973" Program–Research on Theories and Methods of Monitoring and Predicting of Heavy Rainfall in South China under Grant No. 2004CB418300.

†Corresponding author: zhangxiaoh09b@mails.gucas.ac.cn.

(Chinese version published in Vol. 67, No. 1, 2009)

Furthermore, Zhang et al. (2000) conducted a modeling study of mesoscale systems along the Meiyu front in South China. Their model captured the thus 3-D structure of the MCS and a concept model was derived. They inferred that mesoscale systems could induce a meso-low in the lower layer and a meso-high in the upper layer due to the emanation of latent heat. Then the meso-low and meso-high gave positive feedback to the development of the mesoscale systems and strengthened the convective motion. It was suggested that the sensible heat flux, latent heat flux, and PBL process can also affect the development of the strong convective systems (Sun and Zhao, 2000, 2002).

However, there has not existed a general concept of MCS inducing heavy rainfall in South China following current studies and knowledge about severe weather.

In this paper, we aim to analyze the frontal and non-frontal convective clusters in a typical case characterized by a quasi-stationary front in South China on 20 June 2005. Based on GOES-9 satellite cloud-top infrared blackbody temperature, NCEP reanalysis data (1°×1°), Japanese East Asian regional data (20 km) and routine observation networks, the distinction between the frontal and non-frontal systems is summarized in four aspects, namely, dynamic structure (Section 4), convective intensity (Section 5), maintenance mechanism (Section 6), and MPV structure (Section 7).

2. Observational analysis of the rainfall event in South China on 20 June 2005

Figure 1 shows the synoptic setting of the heavy rainfall event that occurred in South China. At 200 hPa (Fig 1a), there was a subtropical anticyclone covering a broad region from the east of the Tibetan Plateau to the east of the South China Sea, and divergent winds were in favor of outflows from convective systems. At 500 hPa (Fig. 1b), the western North Pacific subtropical high (WPSH) developed, and its periphery (identified by the 588 dagpm) extended westward to 110°E. Southwesterlies on the north side of the WPSH indicated that warm moisture was pushed to South China. At 850 hPa (Fig. 1c), a low was

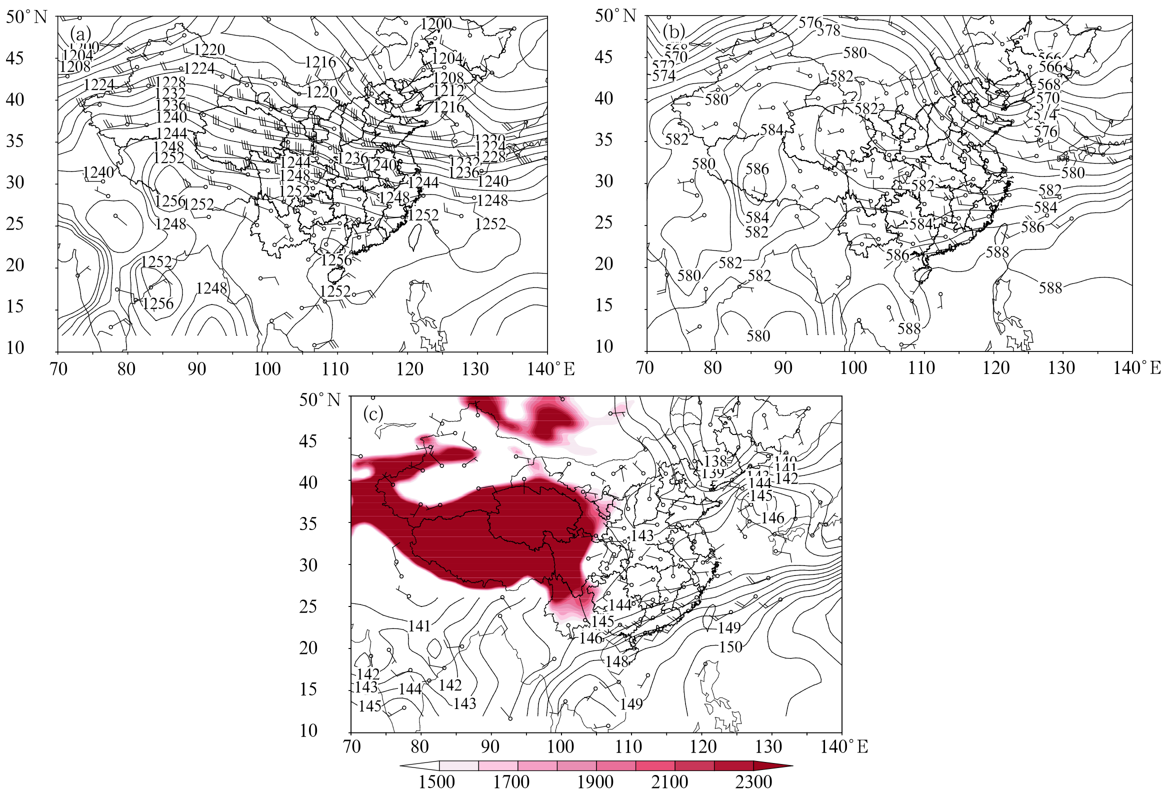

Fig. 1. Geopotential height and wind fields at (a) 200 hPa, (b) 500 hPa, and (c) 850 hPa (unit of contours: dagpm; unit of shaded terrain: m).

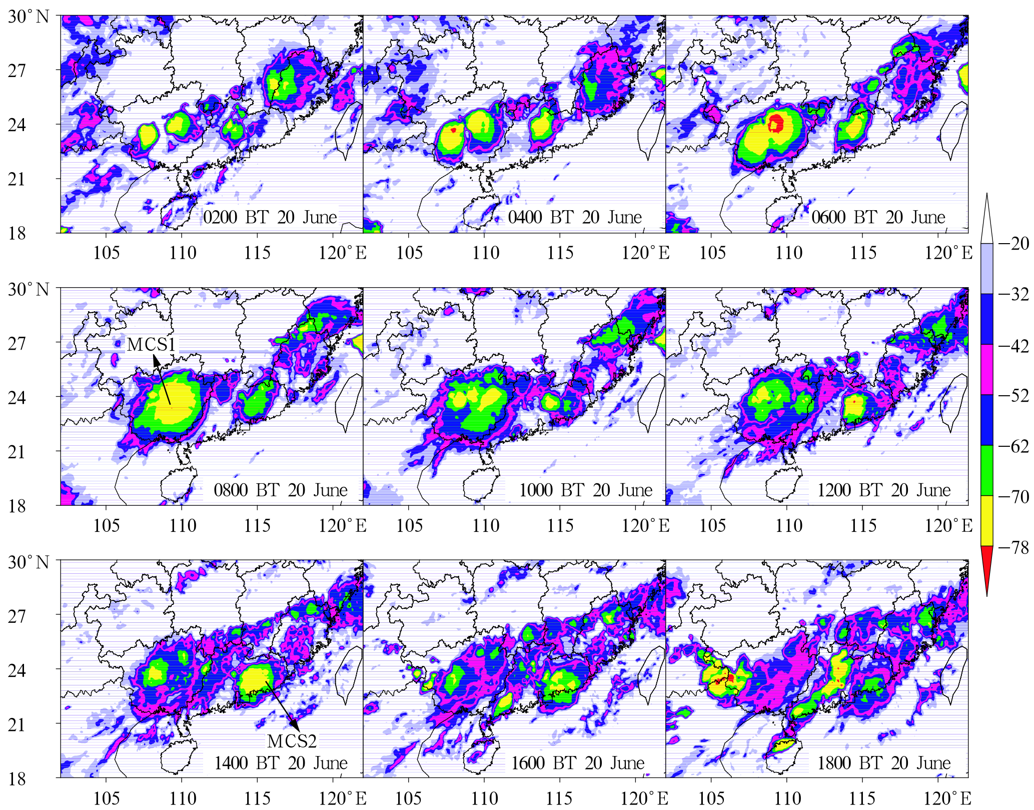

Fig. 2. GOES-9 black body temperature (TBB) evolution every 2 hours (unit: °C).

located over the northeast of Jiangxi, and a trans-meridional shear line was formed near 28°N. The low level jet (LLJ), with the wind speed over 12 m s^{-1}, developed to the south of the shear line. Corresponding to the settings of 850 hPa, there was a quasi-stationary front in South China from surface analysis.

The primary weather systems which induce the heavy rainfall are a vortex at low level, a shear line, and the quasi-stationary front. The synoptic settings from high to low levels advantage the occurrence and development of convection in South China.

3. Temporal variation of two types of meso-scale convective clusters

3.1 Evolution of MCS1 that induced the heavy rainfall in Guangxi

MCS1 was initially formed by two merging clusters, the bigger one of which was not strong enough to meet the definition of MCC at 0200 BT 20 June. By 0600 BT 20 June, the two clusters started to merge, and the cold-shield area of TBB $\leqslant$–32°C reached 1.5×10^5 km^2, and the area of TBB $\leqslant$–52°C was also up to the definition of MCC. Two hours later, MCS1 attained its mature stage, with its area of TBB $\leqslant$–52°C increased to 2.3×10^5 km^2, and it started to induce intense precipitation over the middle of Guangxi. From then on, MCS1 gradually split into a number of meso-β clusters and it dissipated by 1800 BT 20 June. The lifetime of MCS1 was about 10 h from 0600 to 1600 BT 20 June.

3.2 Evolution of MCS2 that induced the heavy rainfall in Guangdong

MCS2 was initiated from the rear of a former cluster at 0900 BT 20 June. Three hours later, MCS2 developed into an MCC, with the cold-shield area of TBB $\leqslant$–32°C reaching 1.02×10^5 km^2. At 1400 BT 20 June, the area of TBB $\leqslant$ –52°C increased to 6.8×10^4 km^2, and then the MCS2 entered its mature stage. From then on, the MCS2 fell to decay and it moved eastward gradually. At 1800 BT 20 June, it migrated to the coastline of Guangdong. Two hours later, MCS2

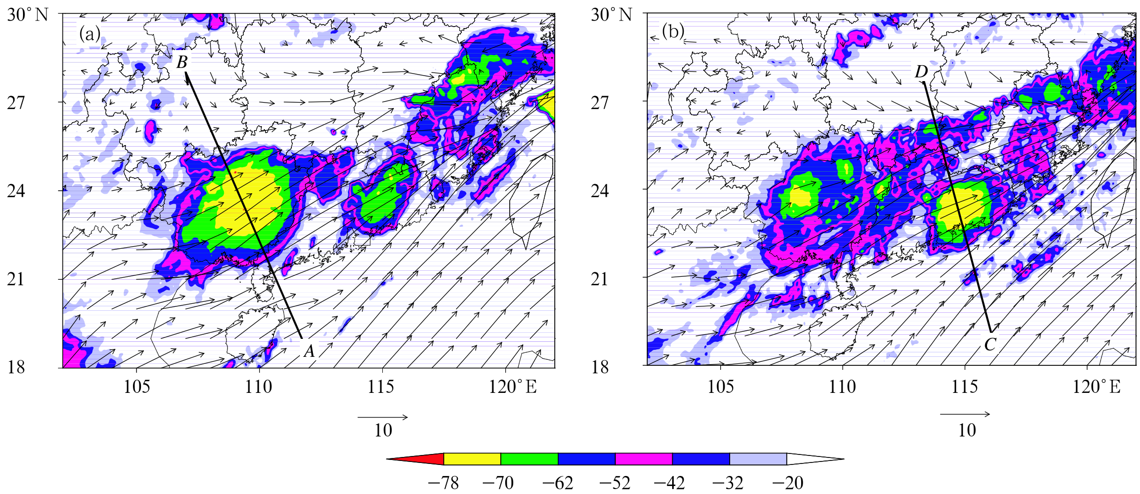

Fig. 3. TBB (shaded) and 850-hPa wind fields at (a) 0800 BT and (b) 1400 BT 20 June 2005. The positions of cross-section AB and CD are highlighted.

dissipated over the sea. The lifetime of MCS2 was about 7 h from 1200 to 1900 BT 20 June.

There are some similar characters between MCS1 and MCS2. Both of them have less than 24-h lifetimes and deep convective centers with TBB ⩽–78°C. However, differences between MCS1 and MCS2 also emerge from observational analyses. Further examinations of these two convective systems are conducted and the comparison between them is documented as follows.

4. Comparison of the dynamic structure between MCS1 and MCS2

Figure 3 shows the low-level wind fields (850 hPa) of MCS1 and MCS2 at their mature stage, respectively. The MCS1 was located near the quasi-stationary front, in which the northerly and southwesterly inflows converged, and the frontal structure of MCS1 was recognizable. Whereas, the MCS2 occurred and developed on the south of the front, the convective region of MCS2 was covered only by southwest airflows in the lower layer, and the non-frontal structure of MCS2 was uncovered.

Figures 4 and 5 show the cross-sections of MCS1 and MCS2 at their mature stage, respectively. A high θ_e tongue (⩾ 350 K) was located on the mid-low levels of MCS1, and the streamlines also indicated the intense updrafts of MCS1 induced by convergence of northerly and southerly winds, which was confirmed

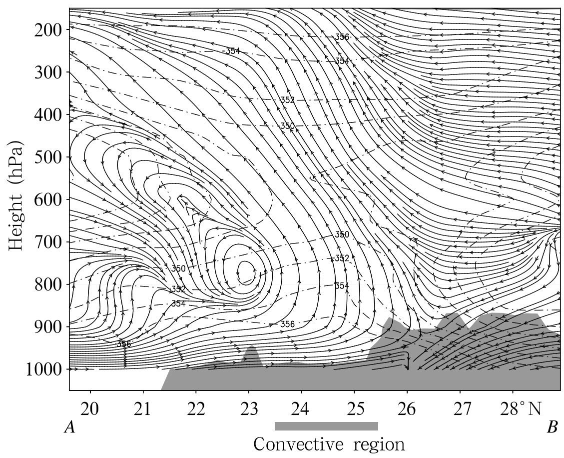

Fig. 4. Streamline (solid) and equivalent potential temperature (dashed point; K) for cross-section AB at 0800 BT 20 June 2005. The terrain is shaded.

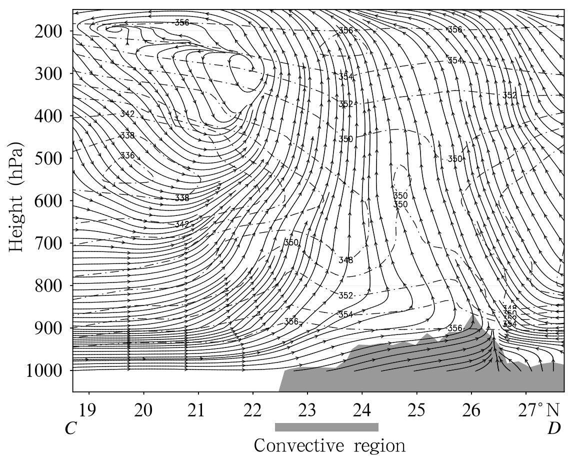

Fig. 5. As in Fig. 4, but for cross-section CD at 1400 BT.

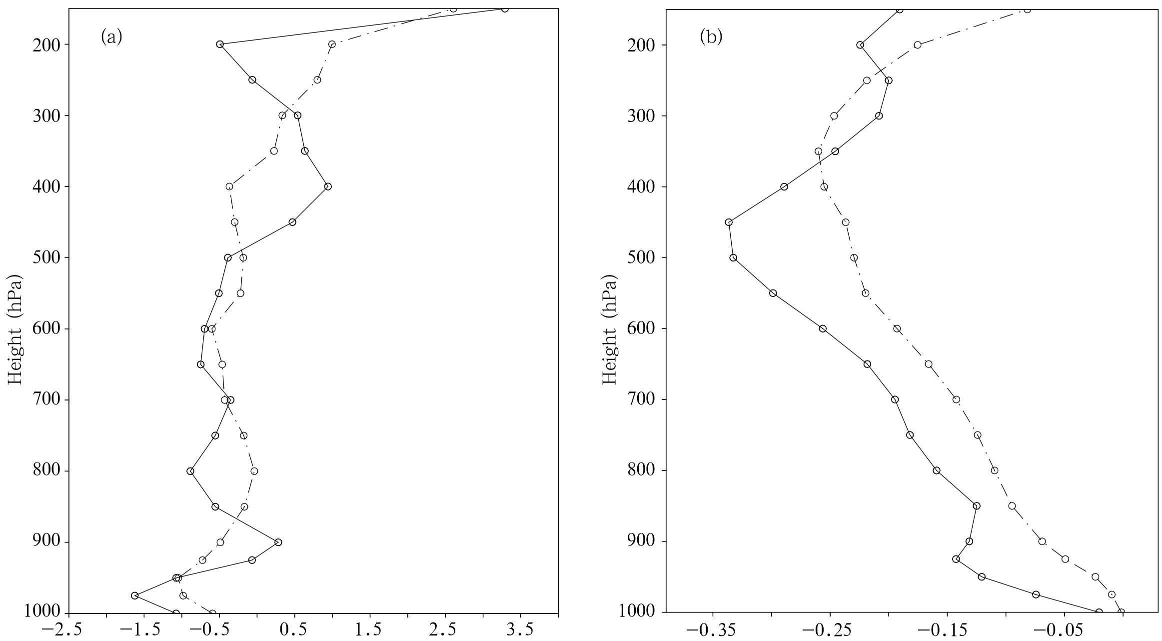

Fig. 6. Averaged profiles of (a) horizontal divergence ($10^{-5}s^{-1}$) and (b) vertical velocity (Pa s^{-1}). Dashed point lines are for MCS1 at 0800 BT, and solid lines for MCS2 at 1400 BT.

from Fig. 3a. In contrast, the vertical motion of MCS2 was the result of orographic effects to the southerly inflows with a high θ_e tongue ($\geqslant$ 350 K), and the non-frontal character was reconfirmed.

In one word, the MCS1 and MCS2 have similar high θ_e tongue in mid-low layer but different dynamic structures which induce vertical motion.

5. Comparison of convective intensity between MCS1 and MCS2

Convective intensity is a main element of mesoscale convective systems. We further examine the intensities of MCS1 and MCS2 with area average of four variables, i.e., horizontal divergence, vertical velocity, moisture flux, and precipitation.

From the area average of horizontal divergence at the mature stage (Fig. 6a), both MCS1 and MCS2 show convergence in the mid-low layer and divergence in the high layer. But the maximum convergence was just 1.0×10^{-5} to $1.5\times10^{-5}s^{-1}$, which was possibly a result during the mature stage of convection and it also implied that the vertical motion would be decreasing from then on.

In addition, the height of naught divergence for MCS1 reached above 400 hPa and was higher than that of MCS2 (500 hPa). It was believed that the northerly inflows in mid-upper layer lifted the height of convergence of MCS1.

At the same time, Fig. 6b shows the vertical velocity profiles of MCS1 and MCS2 at their mature stage. The vertical motions of MCS1 and MCS2 were both updraft, and the velocities were both increasing as height increased in mid-lower layer but decreasing as height increased in upper layer of the troposphere. The vertical motion of MCS1 reached its peak (about –0.26 Pa s^{-1}) at 350 hPa while the velocity of MCS2 culminated (–0.34 Pa s^{-1}) at 450 hPa.

It is then concluded that the pattern of velocity is in accord with the distribution of convergence. It seems that the vertical motion of MCS2 is stronger than that of MCS1. The convective intensity relies not only on the velocity but also on the moisture condition. Therefore, the further analysis below is given mainly from the area average of moisture flux convergence and precipitation.

Figure 7 shows that major moisture flux convergence occurred in lower layer and nearly disappeared at 500 hPa and above because moisture was conveyed mainly by the low-level southwest airflow. The moisture supply of MCS2 seemed more abundant than that of MCS1 in view of the maxima of moisture convergence.

Figure 8 shows that the total precipitation induced by MCS1 from 0200 to 1400 BT 20 June was 79.3 mm, and the total precipitation induced by MCS2 from 0800 to 2000 BT 20 June was 103.11 mm, which was about 24 mm more than that of the former. The difference in precipitation is perhaps was easily thought that because of the difference in the moisture condition.

In summary, the profile of horizontal divergence at the mature stage implies that the vertical motion of MCS1 and MCS2 will become weak from then on.

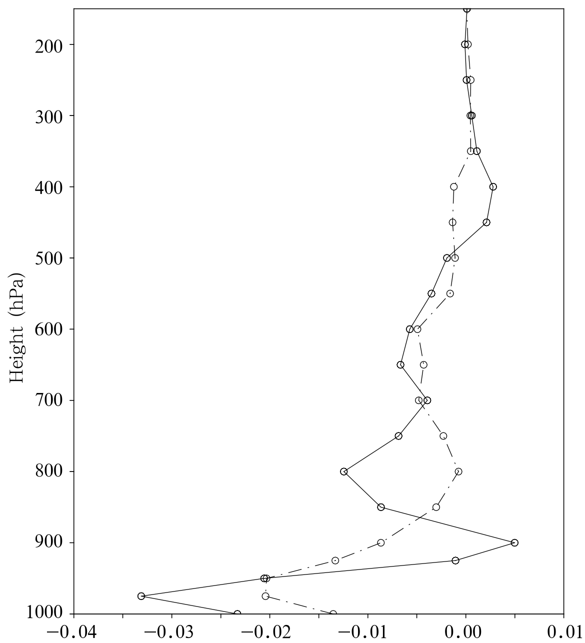

Fig. 7. As in Fig. 6, but for moisture flux divergence (10^{-7}g s^{-1} hPa^{-1}cm^{-2}).

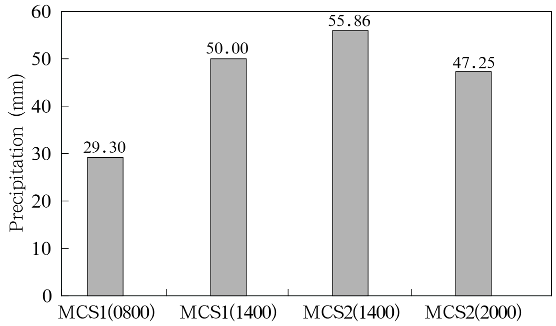

Fig. 8. Histogram of 6-h accumulated precipitation (mm) caused by MCS1 and MCS2, respectively.

And the pattern of vertical velocity is in accord with the distribution of convergence. It seems that the vertical motion of MCS2 is more drastic than that of MCS1. Moreover, the area average of moisture flux convergence and precipitation show that the moisture supply of MCS2 seems more abundant than that of MCS1.

6. Comparison of the maintenance mechanism between MCS1 and MCS2

Generally, the genesis and development of mesoscale cluster are always linked with convective motion, which relies closely on the atmosphere instability, and the intensity of convective motion is to a great extent connected with the instable energy released by the atmosphere.

The MCS1 exhibits slantwise updraft motion while the MCS2 yields vertical updraft motion as shown in Figs. 3 and 4. Whether the different characteristics of converctive motion imply different maintenance mechanisms? We aim to search for the answer to key of that through the following analyses.

6.1 Analysis of the maintenance mechanism for MCS1

The parcel method indicated that the motion of MCS1 (Fig. 9) was from large absolute momentum to small one in lower layer (800 hPa below) of the troposphere, where $\frac{\partial \theta_{\rm e}}{\partial z} < 0$ means inertial stability, and conditional instability. Then the motion got slantwise from small absolute momentum to large one in middle layer where $\frac{\partial \theta_{\rm e}}{\partial z} = 0$, indicating a neutral layer and conditional-symmetric instability.

In the 1980s, Emanuel (1980) and Jascourt et al.(1988) gave the definition of convective-symmetric instability, which is the coexistence of moist-gravity instability (conditional or potential instability) and moist-symmetric instability (conditional or potential-symmetric instability). The pattern of MCS1, which was conditional instability and inertial stability at low levels and conditional-symmetric instability at middle levels, demonstrated that the convective-symmetric

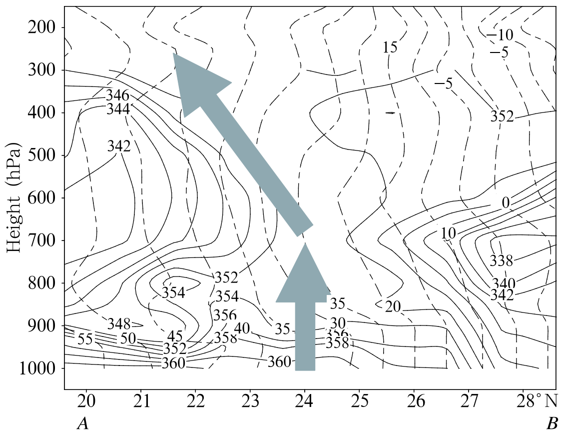

Fig. 9. Equivalent potential temperature (dashed; unit: K) and absolute momentum (solid; with an interval of 5 m s^{-1}) at cross-section AB at 0800 BT. Arrows represent inner upward motions of MCS1.

instability was the maintain mechanism of convective motion.

Cheng and Lu (2006) conducted a modeling study and simulated the evolution and circulation feature of convective-symmetric instability. They found that the circulation would have vertical updrafts at lower levels and slantwise updrafts at upper levels when the conditional instability existed at lower levels and conditional symmetric instability at upper levels. This was again true with the characters of MCS1 in this study. Figures 10 and 11 show the schematic diagram and conceptual model of MCS1 at its mature stage.

6.2 Analysis of the maintenance mechanism for MC-S2

The updrafts of MCS2 (Fig. 10) almost ran parallel with the contours of absolute momentum, and $\frac{\partial\theta_e}{\partial z}<0$ appeared at lower levels. These demonstrate that inertial instability is nonexistent and conditional instability is the main mechanism. The vertical motion of MCS2 is characterized by deep and moist vertical convection.

Deep moist convection has been investigated by Doswell (1987) and Doswell et al. (1996) using the ingredients-based methodology. Instability, moisture, and lifting were thought as three indispensable factors inducing deep moist convection. With reference to Fig. 10, the three factors were all manifested in the convective region of MCS2, and the moist convective ascending inspiried by conditional instability was a unique feature of MCS2.

In addition, the schematic diagram and conceptual model of MCS2 at its mature stage are depicted in Figs. 13 and 14, respectively, which are different from that of MCS1.

At this moment, we can answer the question about whether the different characteristics of convective motion imply different mechanisms. The convective-symmetric instability is the maintaining mechanism for MCS1, represented by slantwise updrafts. Compared with MCS1, the conditional

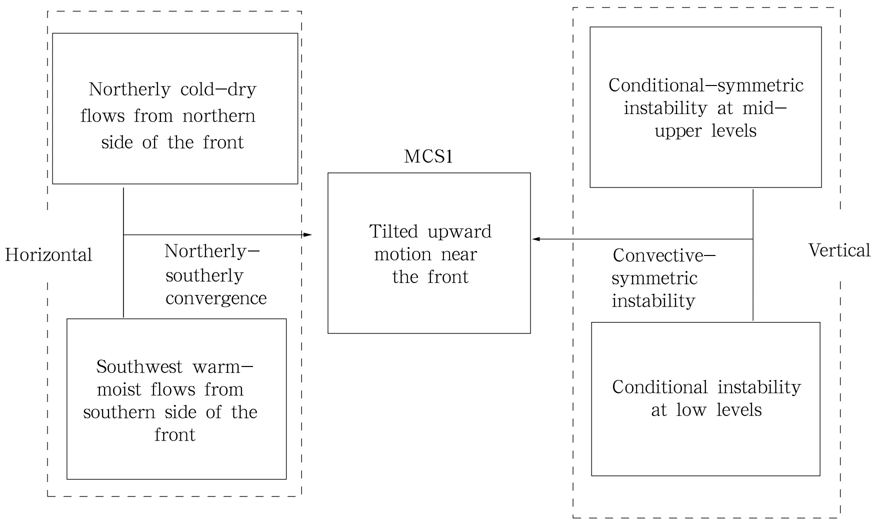

Fig. 10. A schematic diagram for the mature stage MCS1.

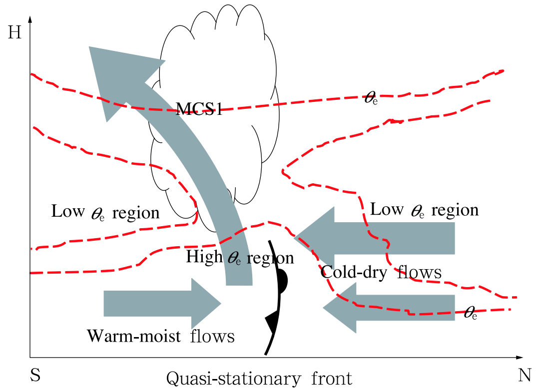

Fig. 11. The conceptual model for the mature stage MCS1.

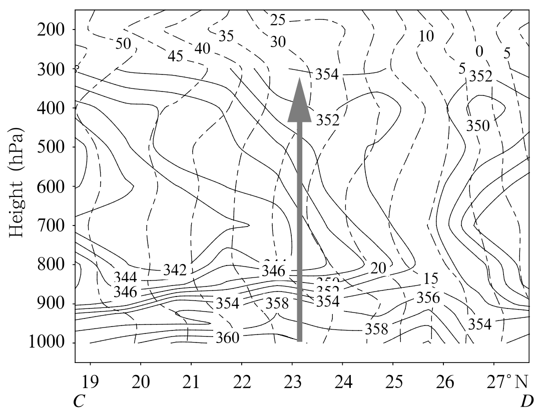

Fig. 12. As in Fig. 9, but for MCS2.

instability is the maintaining mechanism for MCS2, characterized by vertical updrafts.

7. Comparison of moist potential vorticity between MCS1 and MCS2

The definition of MPV (moist potential vorticity) was first mentioned by Bennetts and Hoskins (1979), and was derived by replacing potential temperature with equivalent potential temperature that contains moisture effects. The MPV reflects both dynamic and thermodynamic features of the atmosphere through a combination of inertial instability and convective instability. The diagnosis of MPV helps to reveal real conditions of the atmosphere during rainfall and other convective weathers involving airborne moisture. At the same time, such a PV diagnostic is a useful aid in understanding the relationship between nonhydrostatic moist convection and large-scale balanced flow (Schubert et al., 2001).

There have been many applications of the MPV theory in mesoscale convective weathers in China. A numerical case study of MCSs that developed in South China was carried out by Meng et al. (2004) who found that areas with high pressure and positive moist vorticity were favorable for the development of heavy rainfall and MCS on the slantwise moist isentropic surface. Moreover, Gao et al. (2002) revealed that moist potential vorticity anomaly regions correspond well to the regions of intensive precipitation, from both dynamical and diagnostic methods.

In the following, we want to uncover the MPV

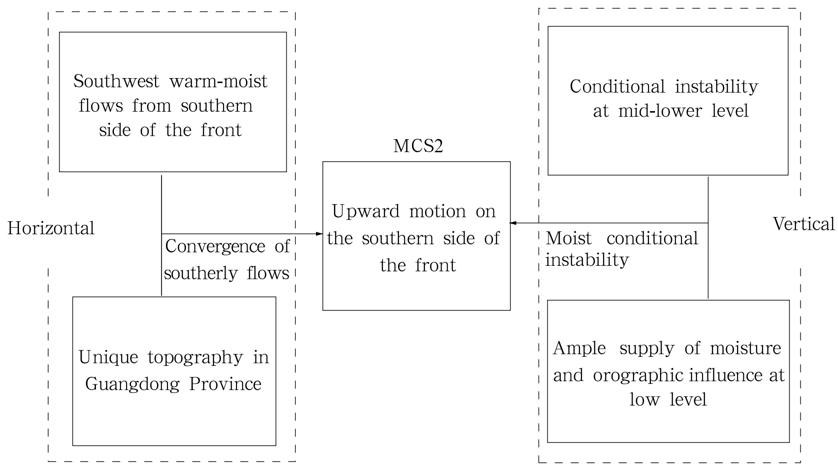

Fig. 13. A schematic diagram for the mature stage MCS2.

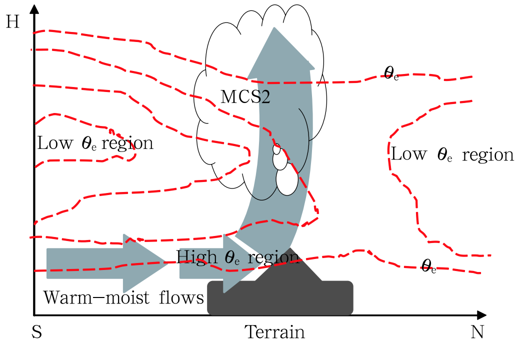

Fig. 14. The conceptual model for the mature stage MCS2.

structure in order to further understand the diffrences between MCS1 and MCS2.

7.1 Description of the MPV theory

Expression of MPV in pressure coordinates is:

$$MPV = -g(f\boldsymbol{k} + \nabla_p \times \boldsymbol{V})\nabla_p\theta_e. \qquad (1)$$

Considering that the horizontal variation of vertical velocity is much less than the vertical shear of horizontal velocities, the former is neglected. The MPV is regarded as a conserved quantity, and the above expression can be written as

$$MPV = -g(\zeta + f)\frac{\partial\theta_e}{\partial p} + g(\frac{\partial v}{\partial p}\frac{\partial\theta_e}{\partial x} - \frac{\partial u}{\partial p}\frac{\partial\theta_e}{\partial y}) = \text{const},$$

where $\zeta = \dfrac{\partial v}{\partial x} - \dfrac{\partial u}{\partial y}$ is relative vorticity and f is geostrophic vorticity. In addition, MPV can also be divided into

$$MPV1 = -g(\zeta + f)\frac{\partial\theta_e}{\partial p},$$
$$MPV2 = g(\frac{\partial v}{\partial p}\frac{\partial\theta_e}{\partial x} - \frac{\partial u}{\partial p}\frac{\partial\theta_e}{\partial y}),$$

where MPV1 is the first component, also named as the vertical component, which depends on the product of vertical absolute vorticity and vertical gradient of equivalent potential temperature; and MPV2 is the second component, also named as the horizontal component, which relies on the vertical shear of winds and horizontal gradient of equivalent potential temperature.

7.2 Comparison of MPV, MPV1, and MPV2

Figure 15 shows the MPV structures of these two convective systems. There both existed negative MPV at mid-lower levels and positive MPV at upper levels. This indicated similar stratification of atmosphere and latent instability in lower layer. But to the north of the convective region, there was positive MPV below 500 hPa in Fig. 15a, which corresponded to the northerly flows in Fig. 4. In contrast to MCS1, MCS2 had negative MPV below 500 hPa in Fig. 15b.

Compared with MPV, MPV1 structure is close to MPV patterns because MPV1 is the main component of MPV, which is about 1 magnitude greater than MPV2.

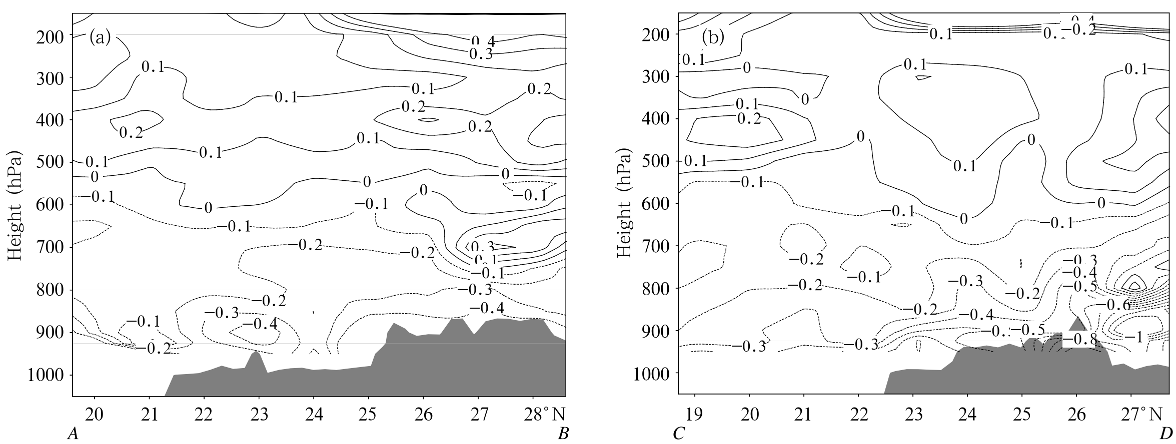

Fig. 15. The moisture potential vorticity (MPV) field for (a) cross-section *AB* of MCS1 at 0800 BT and (b) cross-section *CD* of MCS2 at 1400 BT with an interval of 0.1 PVU ($\times10^{-6}$ m^{2}s^{-1}K kg^{-1}).

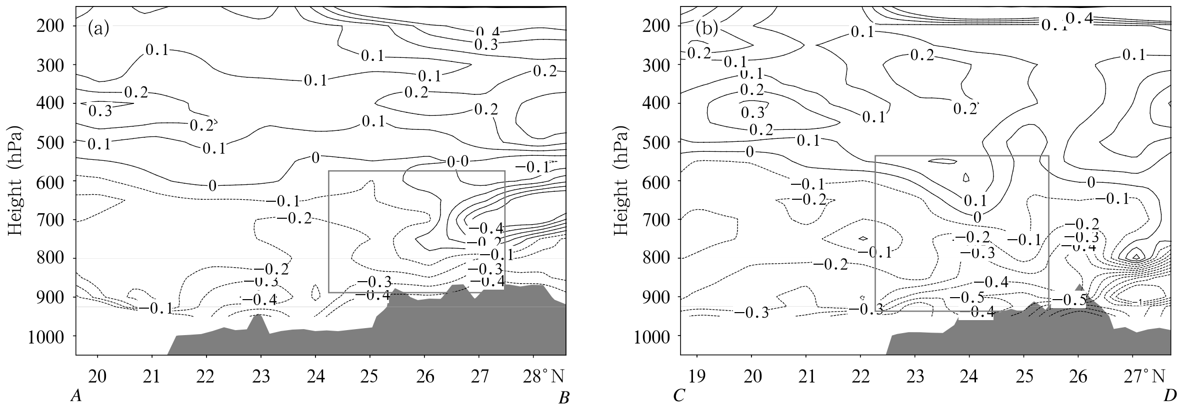

Fig. 16. As in Fig. 15, but for MPV1.

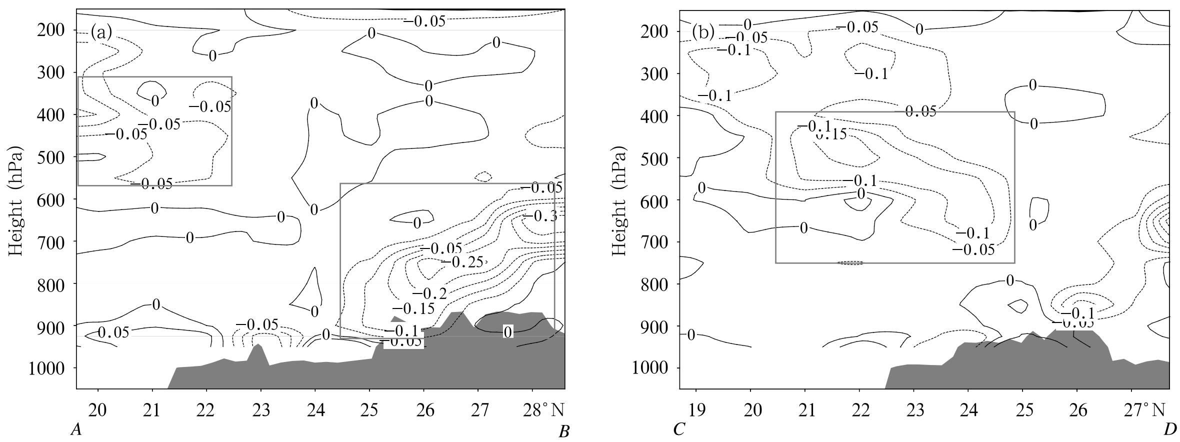

Fig. 17. As in Fig. 15, but for MPV2.

MPV1 is a moist-barotropic term based on its definition. It links together inertial instability $(f+\zeta)$ and convective instability $(-g\frac{\partial\theta_e}{\partial p})$. In the Northern Hemisphere, $(f+\zeta)$ is generally regarded as positive because f is positive (about 10^{-4} s) while ζ is about 10^{-5} s. Then the negative region of MPV1 is thought as convective instability and the area of interface is considered as interaction between dry and wet airflows.

The rectangle in Fig. 16a shows that there was maximum vertical gradient of MPV1 to the north of the convective region, which implies interaction of northerly and southerly airflows in lower layer. Contrary to MCS1, the rectangle in Fig. 16b shows that interaction of wet airflows from mid-lower levels and dry airflows from upper levels.

Additionally, Fig. 17 shows MPV2 structures. It is believed that the negative region of MPV2 is induced by the same positive or negative conditions of $\frac{\partial\theta_e}{\partial y}$ and $\frac{\partial u}{\partial p}$ from the definition of MPV2.

The rectangle in Fig. 17a shows that there were positive $\frac{\partial\theta_e}{\partial y}$ and positive $\frac{\partial u}{\partial p}$ in the south of the convective region and same negative $\frac{\partial\theta_e}{\partial y}$ and $\frac{\partial u}{\partial p}$ in the north of the convective region on the condition that high θ_e tongue was located over the convective region and there existed low level jet (LLJ) and upper levle jet (ULJ) in the south and north of the convective region, respectively.

In the same way, the rectangle in Fig. 17b indicated the same positive $\frac{\partial\theta_e}{\partial y}$ and $\frac{\partial u}{\partial p}$ near the convective region of MCS2.

In this section, the MPV structures of both MCS1 and MCS2 exhibit similar characteristice of latent instability in mid-lower layer, but the MPV1 and MPV2 structures are different in details.

8. Conclusions and discussion

There existed frontal and non-frontal convective clusters that had induced heavy rainfall events in Guangxi and Guangdong, respectively, on 20 June 2005. The two kinds of convective systems have several discrepancies.

MCS1 is located near a quasi-stationary front where the northerly and southwesterly airflows are converged. The convective region of MCS1 presents northerly inflows at middle and higher levels. Whereas MCS2 occurs and develops on the south of the front, and the convective region of MCS2 is covered only by southwest airflows at lower levels.

It seems that the vertical motion of MCS2 is more drastic than that of MCS1. Moreover, the area averages of moisture flux convergence and precipitation show that the moisture supply of MCS2 seems more abundant than that of MCS1. But it is hard to conclude whether the intensity of the frontal convective clusters is stronger than that of the non-frontal systems based on current data in this paper.

Moreover, convective-symmetric instability is the main mechanism for sustained vertical motion of MCS1, and the convective region is featured with slantwise updrafts. On the contrary, conditional instability is the mainteance mechanism of MCS2, characterized by vertical updrafts named as moist deep convection.

Finally, the MPV patterns imply that both of MCS1 and MCS2 have a similar MPV structure with latent instability at mid-lower levels. Distributions of MPV1 indicate that the interaction between cold dry air and warm wet air represents different characters of unstable layers between the MCS1 and MCS2. The different structures of MPV2 demonstrate that high and low-level jets and moisture nearby the convective clusters have different impacts on these two convective systems, respectively.

These conclusions are summarized in Table 1.

Due to limited data interval, the study above just emphasized the diagnosis at the mature stage of the convective systems. Comparison of convective density cannot be generalized by several types of data used in this paper.

Table 1. Comparison of MCS1 and MCS2

	MCS1	MCS2
Dynamic structure	Frontal convective	Non-frontal convective
Maintenance mechanism	Convective-symmetric instability	Conditional instability
Convective intensity	Strong velocity	Stronger velocity
MPV structure	Both with latent instability in mid-lower layer	
MPV1 structure	Interaction of southerly and northerly flows	Interaction of upper and lower flows
MPV2 structure	Represents characters of LLJ and ULJ	Indicates dry air inflows in mid layer

A number of important questions remain to be answered: (1) How are the entire developments of these two kinds of convective systems in detail? (2) Is there any difference between the MCS1 and MCS2 existing before and after the mature stage? (3) Does terrain have any influence on the occurrence and development of convective systems? (4) Are these comparisons implicate to the distribution of precipitation centers? More case studies with detailed mesoscale observations are needed to confirm our results. And high-resolution model simulations are also required to address these questions.

REFERENCES

Bennets, D. A., and B. J. Hoskins, 1979: Conditional symmetric instability–a possible explanation for frontal rain-bands. *Quart. J. Roy. Meteor. Soc.*, **105**(446), 945–962.

Cheng Yanhong and Lu Hancheng, 2006: The evolution and circulation feature of convective-symmetric instability. *Journal of Tropical Meteorology*, **22**(3), 253–258. (in Chinese)

Doswell, C. A. III, 1987: The distinction between large-scale and mesoscale contribution to severe convection: A case study example. *Wea. Forecasting*, **2**, 3–16.

——, H. E. Brooks, and R. A. Maddox, 1996: Flash flood forecasting: An ingredients-based methodology. *Wea. Forecasting*, **11**, 560–581.

Emanuel, K. A., 1980: Forced and free mesoscale motions in the atmosphere. Collection of Lecture Notes on Dynamics of Mesometeorological Disturbances. Proc. CIMMS Symp, Norman, OK, University of Oklahoma/NOAA, 191–259.

Gao Shouting, Lei Ting, and Zhou Yushu, 2002: Diagnostic analysis of moist potential vorticity anomaly in torrential rain systems. *J. Appl. Meteor. Sci.*, **13**(6), 662–670. (in Chinese)

Jascourt, S. D., S. Lindstrom, C. J. Seaman, and D. D. Houghton, 1988: An observation of banded convective development in the presence of weak symmetric stability. *Mon. Wea. Rev.*, **116**, 175–191.

Ji Lingling, Wang Changyu, Jiang Yongqiang, and Kong Yushou, 2004: A case diagnosis of severe convection in the southeast coast region. *Scientia Meteorologica Sinica*, **24**(4), 474–479. (in Chinese)

Jiang Jianying and Ni Yunqi, 2004: Diagnostic study on the structural characteristics of a typical Mei-yu front system and its maintenance mechanism. *Adv. Atmos. Sci.*, **21**(5), 802–813.

Li Jianhui, Zhang Donghua, and Yang Dingqi, 1984: Coastline front in first rainy season of South China and its relationship with heavy rainfall. *Acta Meteor. Sinica*, **42**(3), 370–374. (in Chinese)

Meng Weiguang, Wang Anyu, Li Jiangnan, Fong Soikun, and Hou Erbin, 2004: Moist potential vorticity analysis of the heavy rainfall and mesoscale convective systems in South China. *Chinese J. Atmos. Sci.*, **28**(3), 330–341.

Sun Jianhua and Zhao Sixiong, 2000: A diagnosis and simulation study of a strong heavy rainfall in South China. *Chinese J. Atmos. Sci.*, **24**(3), 381–392.

Sun Jianhu and Zhao Sixiong, 2002: A study of mesoscale convective systems and Its environmental fields during the June 1994 record heavy rainfall in South China. Part II: Effect of physical processes, initial environmental fields and topography on meso-β convective system. *Chinese J. Atmos. Sci.*, **26**(5), 633–646.

Tan Zhemin, Fang Juan, and Wu Rongsheng, 2005: Ekman boundry layer dynamic theories. *Acta Meteor. Sinica*, **63**(5), 543–555. (in Chinese)

Tao Zuyu and Liu Wei, 2005: Discussion on heavy rainfall and moist jet stream. *Acta Meteor. Sinica*, **63**, 825–833. (in Chinese)

Xia Rudi, Zhao Sixiong, and Sun Jianhua, 2006: A study of circumstances of meso-β-scale systems of strong heavy rainfall in warm sector ahead of fronts in South China. *Chinese J. Atmos. Sci.*, **30**(5), 988–1008.

Zhang Bingchen, 1990: *The Study on Heavy Rain in mid-low valley of Yangtze River*. China Meteorological Press, Beijing, 269 pp. (in Chinese)

Zhang Qinghong, Lau Kaihon, Wang Hongqing, and Chen Shoujun, 2000: The simulation of MCS produce by Mei-Yu Front in South China. *Chinese Science Bulletin*, **45**(18), 1988–1992.

Zheng Weizhong, 1990: The symmetric instability of Nanling Mountains stationary front. *Journal of Tropical Meteorology*, **6**, 82–86. (in Chinese)